Journal of Veterinary Science

Original Article
Molecular and Cellular Biology

Check for updates

Epigallocatechin-3-gallate suppresses hemin-aggravated colon carcinogenesis through Nrf2-inhibited mitochondrial reactive oxygen species accumulation

Ju Hyung Seok [1,†], Dae Hyun Kim [1,†], Hye Jih Kim [1,†], Hang Hyo Jo [1],
Eun Young Kim [2], Jae-Hwang Jeong [3], Young Seok Park [4,5,6], Sang Hun Lee [7,8],
Dae Joong Kim [1], Sang Yoon Nam [1], Beom Jun Lee [1,*], Hyun Jik Lee [1,6,*]

[1]College of Veterinary Medicine and Veterinary Medicine Center, Chungbuk National University, Cheongju 28644, Korea
[2]Korea Food Culture Promotion Association, Cheongju 28553, Korea
[3]Department of Biotechnology and Biomedicine, Chungbuk Provincial University, Cheongju 28160, Korea
[4]Department of Neurosurgery, Chungbuk National University Hospital, Cheongju 28644, Korea
[5]Department of Medical Neuroscience, College of Medicine, Chungbuk National University, Cheongju 28644, Korea
[6]Institute for Stem Cell & Regenerative Medicine (ISCRM), Chungbuk National University, Cheongju 28644, Korea
[7]Departments of Biochemistry, Soonchunhyang University College of Medicine, Cheonan 31151, Korea
[8]Medical Science Research Institute, Soonchunhyang University Seoul Hospital, Seoul 04401, Korea

OPEN ACCESS

*Corresponding authors:
Beom Jun Lee
College of Veterinary Medicine and Veterinary Medicine Center, Chungbuk National University, 1 Chungdae-ro, Seowon-gu, Cheongju 28644, Korea.
Email: beomjun@cbu.ac.kr
https://orcid.org/0000-0002-7013-8086

Hyun Jik Lee
College of Veterinary Medicine and Veterinary Medicine Center, Chungbuk National University, 1 Chungdae-ro, Seowon-gu, Cheongju 28644, Korea.
Email: leehyunjik@chungbuk.ac.kr
https://orcid.org/0000-0002-2762-2649

†Ju Hyung Seok, Dae Hyun Kim and Hye Jih Kim equally contributed to this work.

ABSTRACT

Background: Previous studies have presented evidence to support the significant association between red meat intake and colon cancer, suggesting that heme iron plays a key role in colon carcinogenesis. Epigallocatechin-3-gallate (EGCG), the major constituent of green tea, exhibits anti-oxidative and anti-cancer effects. However, the effect of EGCG on red meat-associated colon carcinogenesis is not well understood.
Objectives: We aimed to investigate the regulatory effects of hemin and EGCG on colon carcinogenesis and the underlying mechanism of action.
Methods: Hemin and EGCG were treated in Caco2 cells to perform the water-soluble tetrazolium salt-1 assay, lactate dehydrogenase release assay, reactive oxygen species (ROS) detection assay, real-time quantitative polymerase chain reaction and western blot. We investigated the regulatory effects of hemin and EGCG on an azoxymethane (AOM) and dextran sodium sulfate (DSS)-induced colon carcinogenesis mouse model.
Results: In Caco2 cells, hemin increased cell proliferation and the expression of cell cycle regulatory proteins, and ROS levels. EGCG suppressed hemin-induced cell proliferation and cell cycle regulatory protein expression as well as mitochondrial ROS accumulation. Hemin increased nuclear factor erythroid-2-related factor 2 (Nrf2) expression, but decreased Keap1 expression. EGCG enhanced hemin-induced Nrf2 and antioxidant gene expression. Nrf2 inhibitor reversed EGCG reduced cell proliferation and cell cycle regulatory protein expression. In AOM/DSS mice, hemin treatment induced hyperplastic changes in colon tissues, inhibited by EGCG supplementation. EGCG reduced the hemin-induced numbers of total aberrant crypts and malondialdehyde concentration in the AOM/DSS model.
Conclusions: We demonstrated that EGCG reduced hemin-induced proliferation and colon carcinogenesis through Nrf2-inhibited mitochondrial ROS accumulation.

Generated by xmlinkpress

ORCID iDs
Ju Hyung Seok
https://orcid.org/0000-0003-0002-6158
Dae Hyun Kim
https://orcid.org/0000-0002-8637-8164
Hye Jih Kim
https://orcid.org/0000-0003-0960-1606
Hang Hyo Jo
https://orcid.org/0000-0002-0425-0168
Eun Young Kim
https://orcid.org/0000-0002-9972-664X
Jae-Hwang Jeong
https://orcid.org/0000-0003-3920-3799
Young Seok Park
https://orcid.org/0000-0001-7685-6292
Sang Hun Lee
https://orcid.org/0000-0002-6713-8229
Dae Joong Kim
https://orcid.org/0000-0003-3564-9478
Sang Yoon Nam
https://orcid.org/0000-0001-7576-6543
Beom Jun Lee
https://orcid.org/0000-0002-7013-8086
Hyun Jik Lee
https://orcid.org/0000-0002-2762-2649

Keywords: Hemin; colon cancer; epigallocatechin-3-gallate; reactive oxygen species; oxidative stress; nuclear respiratory factor 2

INTRODUCTION

Colon cancer is the one of leading causes of cancer-associated deaths worldwide and is closely associated with aging and lifestyle factors, such as dietary habits. Among the risk factors for colon cancer, increased red meat intake is considered a critical risk factor that contributes to colon carcinogenesis [1]. Previous studies found that the consumption of processed red meat is closely associated with colon carcinogenesis, suggesting that the heme iron in red meat is a risk factor [2,3]. Epidemiological support the concept that heme iron intake significantly increases the risk of colon cancer [4]. Indeed, a previous study suggested that heme enhances colon carcinogenesis [5]. Heme is the iron-bearing prosthetic group of hemoproteins, such as myoglobin and hemoglobin, in red meat [6]. Because of the stimulatory role of heme in colon cancer occurrence, the regulatory effect and its underlying mechanism have prompted studies into its effects [7].

Hemin is a ferric porphyrin component of hemoglobin, containing a freely exchangeable axial chloride group. It has been used in place of heme delivered from hemoprotein digestion [6,8]. Heme proteins are digested in the upper gastrointestinal tract, delivering heme and ferrous iron oxide to the colon. Heme iron increases mucosal proliferation and cytotoxicity, suggesting that heme has a greater propensity to induce malignancy compared with other forms of dietary iron [5,9]. Several studies have found that the key mechanism of heme iron–induced colon carcinogenesis is oxidative stress-induced lipid peroxidation and gene mutation [10,11]. Because the polyunsaturated fatty acid residues of phospholipids are extremely sensitive to oxidation, lipid peroxidation is initiated by free-radical attack of membrane lipids and is catalyzed by heme [12]. Therefore, these findings indicate that the suppression of heme-induced cellular reactive oxygen species (ROS) may be a potential strategy for preventing or treating colon cancer.

Epigallocatechin-3-gallate (EGCG) is the most abundant polyphenol in green tea and has been studied in various diseases including cancer [13,14]. Previous epidemiological studies suggest an association between green tea consumption and the dose-dependent reduction of mortality associated with cardiometabolic disorders [15]. The beneficial effect of EGCG is due to its anti-oxidative activity. This occurs through the regulation of antioxidant enzyme expression and mitochondrial redox signaling against ROS-induced cellular dysfunction [16]. The semiquinone radical of EGCG reacts with glutathione, which is closely associated with the activation of nuclear factor erythroid-2-related factor 2 (Nrf2) signaling [17]. Although several reports have shown that EGCG suppresses sensitivity to chemotherapy with 5-fluorouracil in colon cancer models, the effect of EGCG on heme-induced colon carcinogenesis has yet to be reported [18]. As heme iron-stimulated lipid peroxidation is mediated by ROS accumulation, EGCG may represent a therapeutic drug for the treatment of heme iron–induced colon cancer [11]. Therefore, we investigated the regulatory effect of EGCG on hemin-induced colon carcinogenesis through modulation of intracellular ROS accumulation in an azoxymethane (AOM) and dextran sodium sulfate (DSS)-induced colon carcinogenesis mouse (AOM/DSS) model and Caco2 colorectal cancer cells.

MATERIALS AND METHODS

Materials

AOM (A5486), hemin (51280), EGCG (E4143), trigonelline hydrochloride (T5506), and MitoTempo (SML 0737) were obtained from Sigma-Aldrich, Inc. (St. Louis, MO, USA). DSS with a molecular weight of 36,000–50,000 was obtained from MP Biomedical Inc. (Santa Ana, CA, USA, MFCD00081551). The colorectal cancer cell line, Caco2, was purchased from the Korean Cell Line Bank (Seoul, Korea). Fetal bovine serum (FBS), phosphate-buffered solution (PBS), and high glucose Dulbecco's Modified Eagle Medium (DMEM) were purchased from HyClone (Logan, UT, USA). Penicillin-streptomycin solution, cell culture dishes, and plates were purchased from Thermo Fisher Scientific Inc. (Waltham, MA, USA). CDK2 (sc-6248), CDK4 (sc-23896), cyclin D (sc-8396), cyclin E (sc-247), and β-actin (sc-47778) primary antibodies were purchased from Santa Cruz Biotechnology (Santa Cruz, CA, USA). Nrf2 (NBP1-32822) and Keap1 (NBP2-03319) antibodies were purchased from Novus Biologicals (Centennial, CO, USA). Horseradish peroxidase-conjugated mouse anti-rabbit secondary antibody and -conjugated mouse IgG kappa binding protein were purchased from Santa Cruz Biotechnology. All mRNA primers were purchased from Cosmogenetech (Seoul, Korea).

Cell culture

Caco2 colorectal cancer cells were cultured in high glucose DMEM (Hyclone), supplemented with 10% FBS (Hyclone) and 1% penicillin-streptomycin solution (Gibco, Grand Island, NY, USA). Caco2 cells were plated in 60 mm dishes or a 96-well plate (Thermo Fisher Scientific Inc.) in a conventional cell incubator (37°C, CO_2 5%, and air 95%). When the cells reached 70% confluency, the medium was changed to serum-free DMEM for 24 h for serum starvation.

Water-soluble tetrazolium salt (WST)-1 cell proliferation assay

The WST-1 cell proliferation assay was performed according to the manufacturer's instructions provided with the EZ-Cytox kit (Daeil Labservice, Seoul, Korea, EZ-1000). Caco2 cells were plated at a density of 1×10^4 cells per well in a 96 well plate. When the cells reached 70% confluency, the media was replaced with serum-free media prior to hemin and EGCG treatment. Cells were incubated in 100 μL of EZ-Cytox reagent with DMEM for 1 h at 37°C. The WST-1 concentration was measured using a Synergy HTX multi-mode microplate reader (BioTek, Winooski, VT, USA).

Trypan blue exclusion assay

Caco2 cells were treated with hemin or EGCG for 48 h. The cells were then washed twice with PBS, trypsinized, and centrifuged at $1,500 \times g$ for 5 min. The pellet was suspended with 0.4% trypan blue solution (Sigma-Aldrich, T8154). The cell number and viability were measured using a Countess II automated cell counter (Thermo Fisher Scientific Inc.).

Measurements of intracellular and mitochondrial ROS

The DCF-DA (Thermo Fisher Scientific Inc., C6821) and MitoSOX (Thermo Fisher Scientific Inc., M36008) assays were used to determine intracellular ROS and mitochondrial-specific ROS levels in Caco2 cells, respectively. The DCF-DA and MitoSOX staining assays were performed according to the manufacturer's instructions. The detailed experimental protocols were previously described [19]. The fluorescence intensities of DCF-DA and MitoSOX were detected using a Synergy HTX multi-mode microplate reader (BioTek).

Lactate dehydrogenase (LDH) cytotoxicity assay

Caco2 cells were plated at a density of 1×10^4 cells per well in a 96-well plate. When cell confluency reached 70%, the media was replaced with serum-free media prior to drug treatment. After incubation with hemin or EGCG, the media was collected and centrifuged at $600 \times g$ for 10 min. The supernatant was collected and the LDH cytotoxicity assay was performed following the manufacturer's instructions provided with the EZ-LDH kit (DoGenBio, Seoul, Korea, DG-LDH500). The LDH release level was measured using a Synergy HTX multi-mode microplate reader (BioTek).

Western blot analysis

Harvested Caco2 cells were washed with cold PBS and mixed with RIPA lysis buffer (Atto, Tokyo, Japan). The detailed experimental protocols were previously described [19]. Uncropped representative blot images are described in **Supplementary Figs. 1-6**.

Real-time quantitative polymerase chain reaction (PCR)

Harvested Caco2 cells were lysed with RL buffer and dithiothreitol solution. The RNA was extracted using an RNA extraction kit (Takara, Tokyo, Japan). The RNA extraction and quantitative PCR were performed according to the manufacturer's instructions. The detailed experimental protocols were previously described [19]. The relative expression of target mRNA was normalized to *ACTB* mRNA. All sequences of mRNA primer are described in **Supplementary Table 1**.

Animals

Male Institute for Cancer Research (ICR) mice were obtained from Orient Bio (Seongnam, Korea) and housed in an isolated polycarbonate cage (5 mice/cage) and specific pathogen free laboratory condition. The temperature and relative humidity were set at 20°C ± 2°C and 50% ± 20%, respectively. Light and dark cycles were set at 12 h each and the intensity of illumination was maintained at 150–300 lux. An AIN-76A purified diet was obtained from Central Laboratory Animal Inc. (Seoul, Korea). During the experimental period, diets and litter were all used after sterilization. The animal experiments were conducted in compliance with the "Guide for Care and Use of Laboratory Animals" of Chungbuk National University (CBNUR-1102-17).

Experimental design

Male ICR mice (4-week-old) were acclimated to the cage for a week, then divided into three groups: carboxymethylcellulose (CMC; control group), hemin treatment (hemin group), and hemin with EGCG co-treatment (hemin + EGCG group). Hemin (2 g/kg) mixed with 1% CMC was orally administered to the hemin group and the hemin + EGCG group. The hemin + EGCG group was provided with distilled water containing EGCG (0.1%, ad libitum). Then, AOM (10 mg/kg) was subcutaneously injected three times into the mice at day 0 and after the first and second weeks of the experimental period to induce the formation of preneoplastic lesions in the colon. On the second week of the experimental period, distilled water containing 2% DSS was given to the mice for 7 days.

Aberrant crypt foci (ACF) and aberrant crypt (AC) assay

Colons were harvested, flushed with saline, opened longitudinally, and fixed flat between filter paper in 10% neutral buffered formalin. The formalin-fixed tissues were stained with 0.2% methylene blue solution for a few seconds. The total number of ACF and AC in each focus was counted under a microscope. ACF were identified with following morphological

characteristics: 1) enlarged and elevated crypts compared with the normal mucosa and 2) increased pericryptal space and irregular lumens.

Thiobarbituric acid reactive substance (TBARS) assay

Dry feces were collected under each cage of five mice 24 h before sacrifice. Samples were prepared by adding 1 mL of distilled water to 0.3 g of dried feces. Samples were incubated at 37°C for an hour and thoroughly mixed during incubation. Following centrifugation for 15 min at 20,000 × g, the supernatant was collected and stored at −20°C until use. Malondialdehyde (MDA) levels were measured using a TBARS Assay Kit (Cayman Chemical, Ann Arbor, MI, USA). The method is based on the reaction of thiobarbituric acid with MDA under high temperature (90°C–100°C) and the resultant color was measured at 530 nm.

Statistical analysis

Data are expressed as the means ± SE of the mean. Data were analyzed with a one-way analysis of variance followed by Holm-Sidak test. The differences were determined to be significant at $p < 0.05$. All statistical tests were performed and analyzed using SigmaPlot program (Systat Software, Inc., San Jose, CA, USA).

RESULTS

Stimulatory effects of hemin on proliferation and mitochondrial ROS accumulation in Caco2 cells

We examined the regulatory effect of hemin on the survival and proliferation of Caco2 colorectal cancer cells. Using trypan blue exclusion and LDH assays, we observed that hemin treatment (100 nM, 1 μM, and 10 μM) did not affect cell viability or LDH release levels (**Fig. 1A and B**). However, the number of Caco2 cells treated with hemin (1 μM and 10 μM) was higher compared with that of Caco2 cells treated with vehicle or 100 nM of hemin (**Fig. 1C**). Similarly, the WST-1 assay revealed that both 1 μM and 10 μM of hemin significantly increased WST-1 levels (**Fig. 1D**). In addition, we confirmed that hemin treatment increased the expression of the cell cycle regulatory proteins, CDK2, CDK4, cyclin D, and cyclin E (**Fig. 1E**). These findings indicate that hemin treatment stimulates cell proliferation, but not survival, in Caco2 cells.

To determine the effect of hemin treatment on ROS accumulation in Caco2 cells, we used DCF-DA intracellular ROS detection and MitoSOX mitochondrial ROS detection assays. As shown in the **Fig. 2A and B**, both 1 μM and 10 μM of hemin treatment significantly increased intracellular and mitochondrial ROS levels in Caco2 cells. In addition, the superoxide scavenger, MitoTEMPO pretreatment suppressed hemin-induced WST-1 levels and the cell cycle regulatory proteins, CDK2, CDK4, cyclin D, and cyclin E (**Fig. 2C and D**). Collectively, the data indicate that hemin-induced mitochondrial ROS accumulation is important for Caco2 proliferation.

Suppression of EGCG on hemin-induced Caco2 proliferation through Nrf2 activation

To determine the effect of EGCG on colorectal cancer cells with hemin, we pretreated 1 μM of EGCG to Caco2 cells prior to 1 μM of hemin treatment. EGCG pretreatment suppressed the hemin-indued increase in cell number and WST-1 levels (**Fig. 3A and B**). EGCG reversed hemin-induced expression of the cell cycle regulatory proteins, CDK2, CDK4, cyclin D, and cyclin E (**Fig. 3C**). Using a mitochondrial ROS detection assay, we found that EGCG
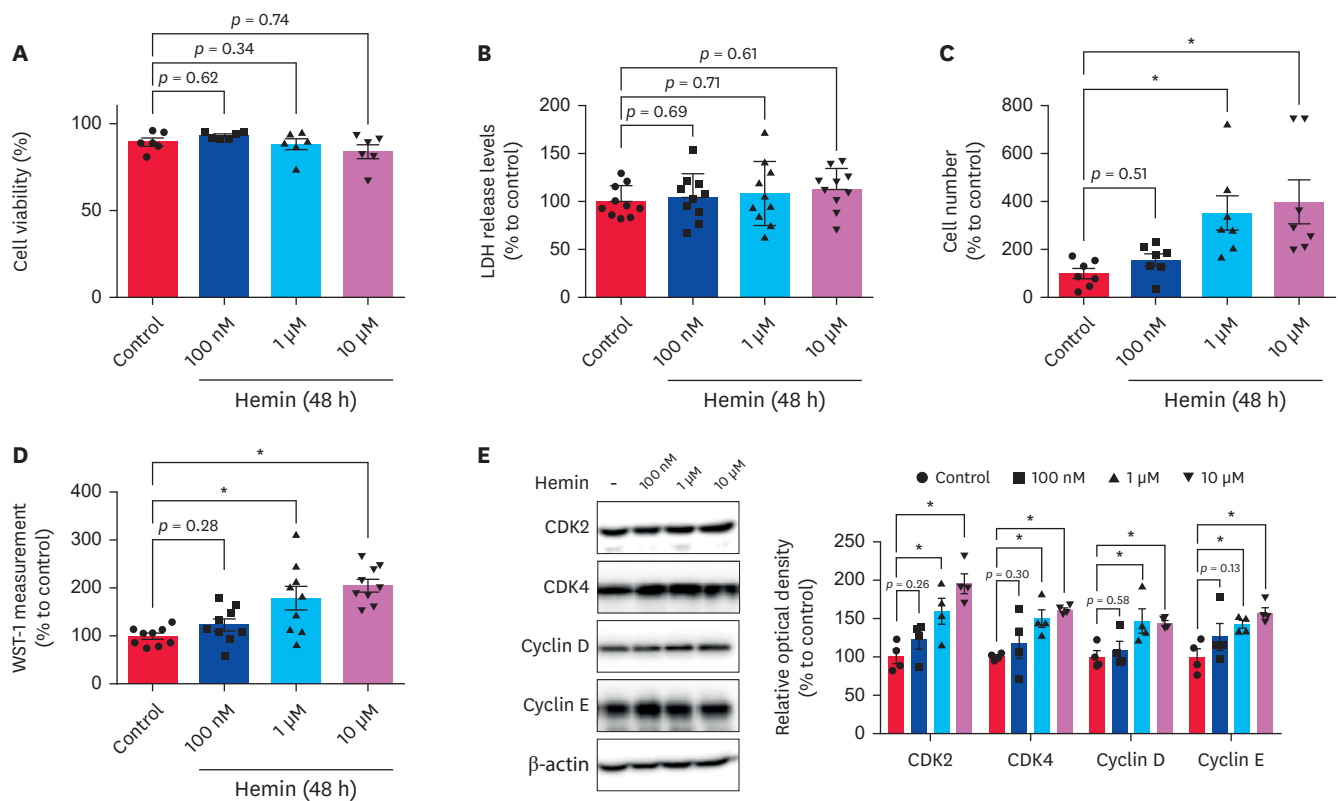
Fig. 1. Effect of hemin on the proliferation in Caco2 cells. Caco2 cells were treated with hemin (100 nM, 1 μM, and 10 μM) for 48 h. (A) Cell viability of hemin-treated Caco2 cells was measured using the trypan blue exclusion assay (n = 6). (B) LDH released from apoptotic cells in cell-conditioned media was detected by LDH assay (n = 9). (C) Cell number of hemin-treated Caco2 cells was analyzed by trypan blue exclusion assay (n = 7; p = 0.013: Control vs. Hemin 1 μM; p = 0.005: Control vs. Hemin 10 μM). (D) WST-1 levels were measured by a WST-1 cell proliferation assay (n = 9; p = 0.002: Control vs. Hemin 1 μM; p < 0.001: Control vs. Hemin 10 μM). (E) CDK2, CDK4, cyclin D, cyclin E, and β-actin expression levels were measured by western blot analysis (n = 4; p = 0.015: Control vs. Hemin 1 μM CDK2; p < 0.001: Control vs. Hemin 10 μM CDK2; p = 0.019: Control vs. Hemin 1 μM CDK4; p < 0.008: Control vs. Hemin 10 μM CDK4; p = 0.027: Control vs. Hemin 1 μM cyclin D1; p = 0.026: Control vs. Hemin 10 μM cyclin D1; p = 0.039: Control vs. Hemin 1 μM cyclin E; p = 0.011; Control vs. Hemin 10 μM cyclin E). Quantitative data are presented as the mean ± SE of the mean with scatter plots.
LDH, lactate dehydrogenase; WST, water-soluble tetrazolium salt.
*p < 0.05.

pretreatment reversed hemin-induced mitochondrial ROS levels in Caco2 cells (**Fig. 3D**). Furthermore, we investigated the effects of pre, simultaneous and post treatments of EGCG on proliferation and mitochondrial oxidative stress in Caco2 cells incubated with hemin. Our data showed that the WST-1 levels and mitochondrial ROS levels in both simultaneous and post treatments of EGCG groups were similar to those of pre-treatment of EGCG group (**Supplementary Fig. 7**). These findings indicate that EGCG suppresses hemin-increased proliferation and mitochondrial ROS accumulation in Caco2 cells.

It has been reported that EGCG acts as a potent inducer of Nrf2; therefore, we examined the regulatory effect of EGCG on Nrf2 expression in hemin-treated Caco2 cells. We found that hemin treatment increased Nrf2 expression, but decreased Keap1 expression in a time-dependent manner (**Fig. 4A**). Furthermore, we investigated the effect of Nrf2 inactivation on hemin-induced mitochondrial ROS accumulation. Our data showed that trigonelline, a Nrf2 inhibitor, further increased hemin-induced mitochondrial ROS levels in Caco2 (**Supplementary Fig. 8**). EGCG pretreatment augmented hemin-induced Nrf2 expression (**Fig. 4B**); however, EGCG pretreatment did not affect hemin-reduced Keap1 expression (**Fig. 4B**). To determine whether EGCG-induced Nrf2 activation, we measured the expression of several Nrf2-targeted
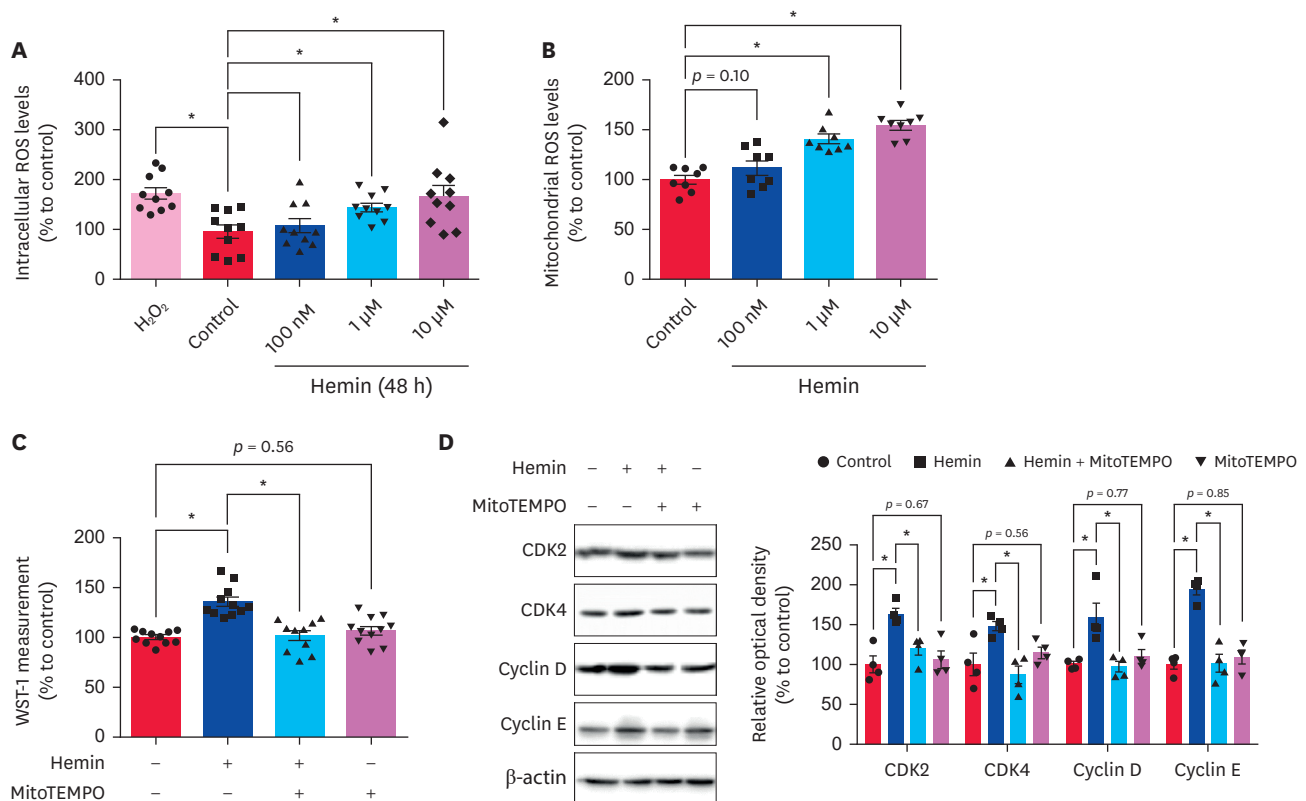
Fig. 2. Role of hemin in mitochondrial ROS in Caco2 cells. (A, B) Caco2 cells were treated with hemin (100 nM, 1 μM, and 10 μM) for 48 h. (A) Cells were pretreated with hydrogen peroxide (H_2O_2, 100 μM) for 4 h prior to hemin treatment (1 μM) for 48 h. Intracellular ROS levels were determined by DCF-DA staining. H_2O_2 treatment was used as a positive control for analysis (n = 10; p = 0.002: Control vs. H_2O_2; p = 0.042: Control vs. Hemin 1 μM; p = 0.003: Control vs. Hemin 10 μM). (B) Mitochondrial ROS levels were analyzed by the MitoSOX staining assay (n = 8). (C, D) Cells were pretreated with MitoTEMPO (1 μM) for 30 min prior to hemin treatment (1 μM) for 48 h (p < 0.001: Control vs. Hemin 1 μM; p < 0.001: Control vs. Hemin 10 μM). (C) WST-1 levels were measured by the WST-1 cell proliferation assay (n = 11; p < 0.001: Control vs. Hemin; p < 0.001: Control vs. Hemin + MitoTempo). (D) CDK2, CDK4, cyclin D, cyclin E, and β-actin protein expression was determined by western blot analysis (n = 4; p = 0.003: Control vs. Hemin CDK2; p = 0.027: Control vs. Hemin + MitoTempo CDK2; p = 0.031: Control vs. Hemin CDK4; p = 0.007: Control vs. Hemin + MitoTempo CDK4; p = 0.008: Control vs. Hemin cyclin D; p = 0.007: Control vs. Hemin + MitoTempo cyclin D; p < 0.001: Control vs. Hemin cyclin E; p < 0.001: Control vs. Hemin + EGCG cyclin E). Quantitative data are presented as the mean ± SE of the mean with scatter plots. ROS, reactive oxygen species; WST, water-soluble tetrazolium salt; EGCG, epigallocatechin-3-gallate.
*p < 0.05.

genes by quantitative real time-PCR. The expression of *GPX2*, *GLRX1*, and *SOD2* mRNA in EGCG-pretreated Caco2 cells treated with hemin was higher compared with Caco2 cells treated with hemin alone (**Fig. 4C**). To identify the role of EGCG-induced Nrf2 in Caco2 cell proliferation under high hemin conditions, we pretreated the cells with the Nrf2 inhibitor, trigonelline. We observed that trigonelline treatment reversed EGCG-suppressed WST-1 levels and cell cycle regulatory protein expression (**Fig. 4D and E**). Taken together, we demonstrated that EGCG augmented hemin-induced Nrf2 expression, which plays an important role in the suppression of mitochondrial ROS accumulation in Caco2 cells.

Inhibitory effect of EGCG supplementation on hemin-induced colonic neoplasia in the AOM/DSS mouse model

To investigate the effects of hemin and EGCG on colon carcinogenesis *in vivo*, we evaluated EGCG and hemin in an AOM/DSS model of colitis-associated colorectal cancer (CAC, **Fig. 5A**). This model has been used as a robust, reproducible colon carcinogenesis model for human CAC studies. The body weight of the mice were measured every week to confirm the effects of hemin and EGCG. The body weight for all groups increased with time; however, there were no
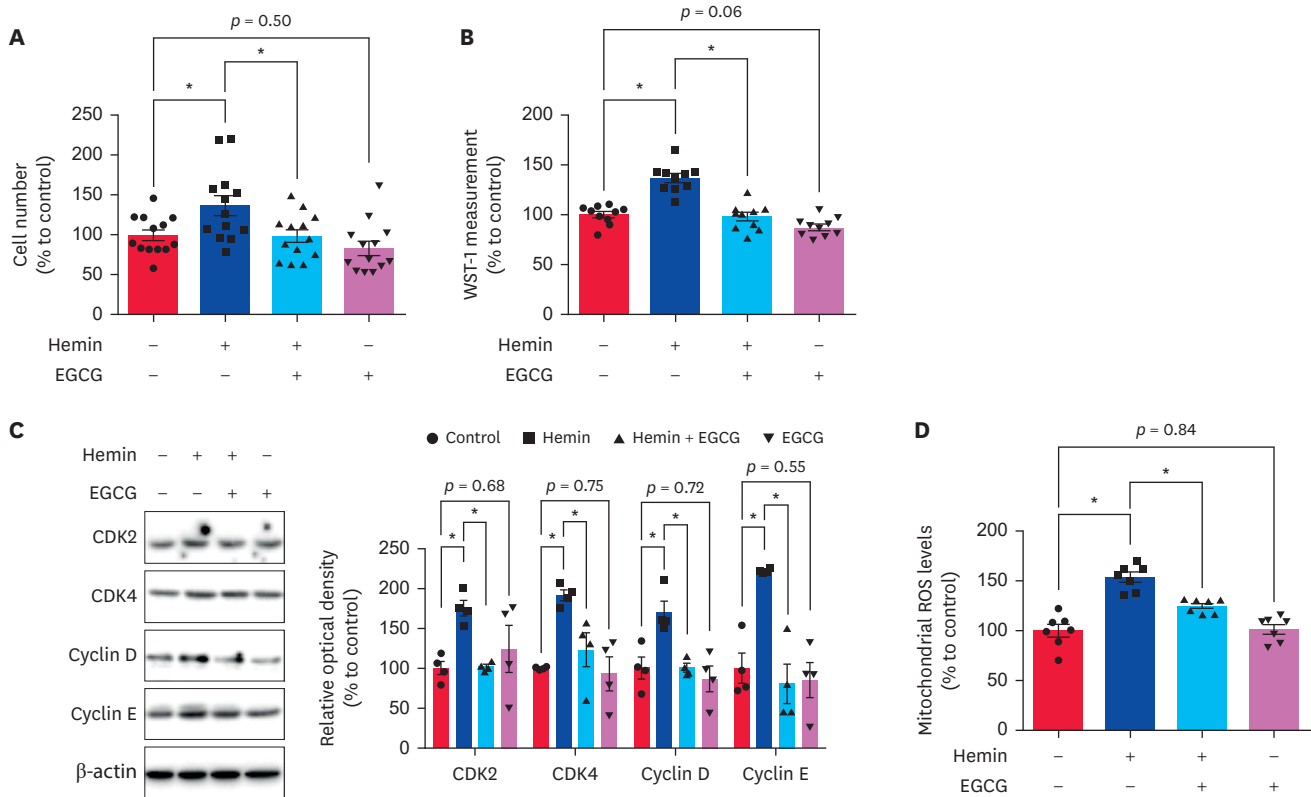
Fig. 3. Effect of EGCG on hemin-induced proliferation and mitochondrial ROS in Caco2 cells. Caco2 cells were treated with EGCG for 30 min prior to hemin exposure (1 μM) for 48 h. (A) Cell number was analyzed by using trypan blue exclusion assay (n = 13; p = 0.028: Control vs. Hemin; p = 0.026: Control vs. Hemin + EGCG). (B) WST-1 levels were measured by using WST-1 cell proliferation assay (n = 10; p < 0.001: Control vs. Hemin; p < 0.001: Control vs. Hemin + EGCG). (C) CDK2, CDK4, cyclin D, cyclin E, and β-actin protein expressions were measured by western blot analysis (n = 4; p = 0.038: Control vs. Hemin CDK2; p = 0.037: Control vs. Hemin + EGCG CDK2; p = 0.006: Control vs. Hemin CDK4; p = 0.033: Control vs. Hemin + EGCG CDK4; p = 0.011: Control vs. Hemin cyclin D; p = 0.010: Control vs. Hemin + EGCG cyclin D; p = 0.003: Control vs. Hemin cyclin E; p = 0.001: Control vs. Hemin + EGCG cyclin E). (D) Mitochondrial ROS levels of Caco2 treated with hemin or EGCG were analyzed by MitoSOX staining assay (n = 7; p < 0.001: Control vs. Hemin; p = 0.002: Control vs. Hemin + EGCG). Quantitative data are presented as a mean ± SE of the mean with scatter plots.

ROS, reactive oxygen species; WST, water-soluble tetrazolium salt; EGCG, epigallocatechin-3-gallate.

*p < 0.05.

statistically significant difference between the experimental groups (**Fig. 5B**). To determine the effect of hemin and EGCG on colon carcinogenesis histologically, we investigated neoplastic change of colon tissues in AOM/DSS mice. ACF are the earliest morphological alteration observed during the development of colonic mucosal neoplasia and is extensively used to identify modulators of colon carcinogenesis. Previous studies on the morphological and molecular features of ACF support the contention that ACF are putative preneoplastic lesions that may serve as biomarkers for colon cancer. Therefore, we counted the total numbers of AC and ACF lesions in colon tissues to determine the effects of EGCG and hemin on neoplastic changes in the AOM/DSS model. The total number of ACF in the hemin group was significantly increased compared with the control group. In addition, the total number of ACF in the hemin + EGCG group was significantly decreased compared with that in hemin group (**Fig. 5C and D**). An AC assay revealed that the total number of AC in the hemin group was increased compared with the control group. In addition, the total number of AC in the hemin + EGCG group was decreased compared with the hemin group (**Fig. 5E**). Lipid peroxidation of the metabolite MDA in feces is a marker for oxidative stress in colonic mucosa. We measured MDA concentrations in feces using the TBARS assay. As shown in **Fig. 5F**, TBARS concentration in the hemin group was significantly increased compared
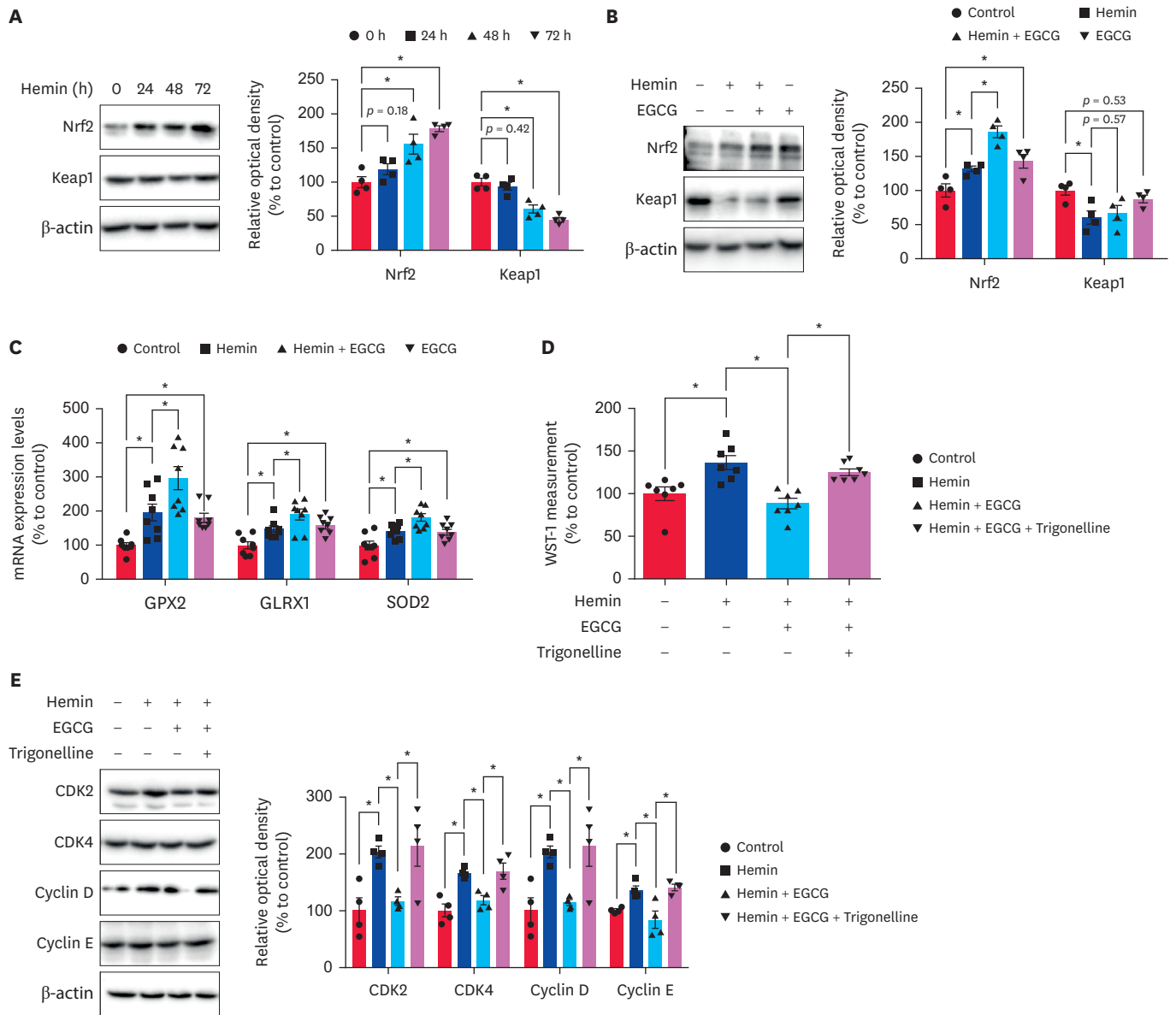
Fig. 4. Role of EGCG-regulated Nrf2 in hemin-induced proliferation in Caco2 cells. (A) Caco2 cells were treated with hemin (100 nM, 1 μM, and 10 μM) for 48 h. Nrf2, Keap1 and β-actin protein expression were measured by western blot analysis (n = 4; p = 0.005: Control vs. Hemin 48 h Nrf2; p < 0.001: Control vs. Hemin 72 h Nrf2; p < 0.001: Control vs. Hemin 48 h Keap1; p < 0.001: Control vs. Hemin 72 h Keap1). (B, C) Cells were pretreated with EGCG (1 μM) for 30 min prior to hemin exposure (1 μM) for 48 h. (B) Nrf2, Keap1, and β-actin protein expression were determined by western blot analysis (n = 4; p = 0.040: Control vs. Hemin Nrf2; p = 0.003: Control vs. Hemin + EGCG Nrf2; p = 0.012: Control vs. EGCG Nrf2; p = 0.035: Control vs. Hemin Keap1). (C) The expression of *GPX2*, *GLRX1*, and *SOD2* mRNA were measured in Caco2 cells following hemin or EGCG treatment (n = 8; p = 0.014: Control vs. Hemin *GPX2*; p = 0.014: Control vs. Hemin + EGCG *GPX2*; p = 0.033: Control vs. EGCG *GPX2*; p = 0.027: Control vs. Hemin *GLRX1*; p = 0.033: Control vs. Hemin + EGCG *GLRX1*; p = 0.006: Control vs. EGCG *GLRX1*; p = 0.023: Control vs. Hemin *SOD2*; p = 0.027: Control vs. Hemin + EGCG *SOD2*; p = 0.020: Control vs. EGCG *SOD2*). (D, E) Cells were pretreated with trigonelline (10 μM) for 30 min prior to hemin (1 μM) or EGCG (1 μM) treatment for 48 h. (D) WST-1 levels were measured by the WST-1 cell proliferation assay (n = 7; p = 0.003: Control vs. Hemin; p < 0.001: Control vs. Hemin + EGCG; p = 0.003: Hemin + EGCG vs. Hemin + EGCG + Trigonelline). (E) The expression of CDK2, CDK4, cyclin D, cyclin E, and β-actin protein was measured by western blot analysis (n = 4; p = 0.031: Control vs. Hemin CDK2; p = 0.049: Control vs. Hemin + EGCG CDK2; p = 0.035: Hemin + EGCG vs. Hemin + EGCG + Trigonelline CDK2; p = 0.003: Control vs. Hemin CDK4; p = 0.019: Control vs. Hemin + EGCG CDK4; p = 0.016: Hemin + EGCG vs. Hemin + EGCG + Trigonelline CDK4; p = 0.030: Control vs. Hemin cyclin D; p = 0.041: Control vs. Hemin + EGCG cyclin D; p = 0.029: Hemin + EGCG vs. Hemin + EGCG + Trigonelline cyclin D; p = 0.042: Control vs. Hemin cyclin E; p = 0.007: Control vs. Hemin + EGCG cyclin E; p = 0.004: Hemin + EGCG vs. Hemin + EGCG + Trigonelline cyclin E). Quantitative data are presented as the mean ± SE of the mean with scatter plots.
WST, water-soluble tetrazolium salt; EGCG, epigallocatechin-3-gallate; Nrf2, nuclear factor erythroid-2-related factor 2.
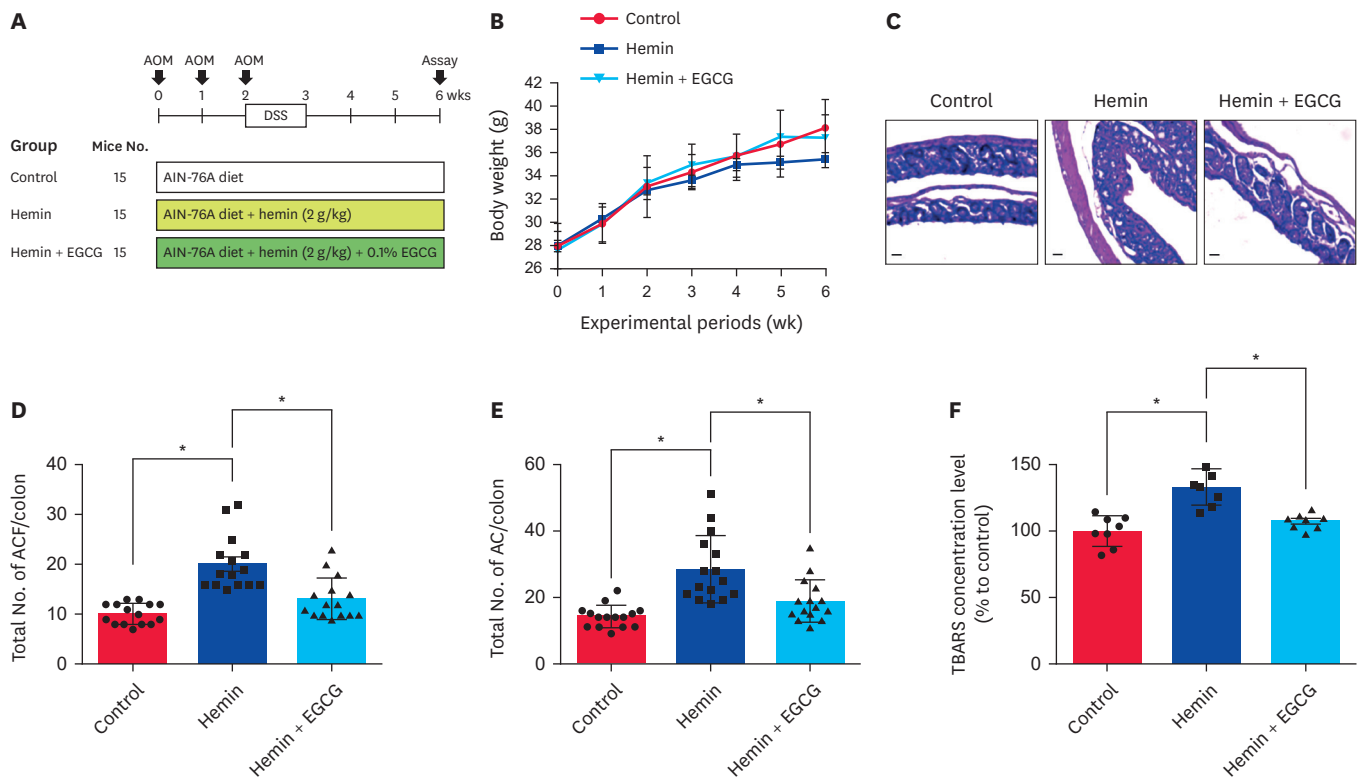*p < 0.05.

Fig. 5. Effect of EGCG supplementation on hemin-induced colon carcinogenesis in the AOM/DSS model. (A-E) After acclimation for 1 week-old, 5-week-old male ICR mice were administered weekly subcutaneous injections of AOM (10 mg/kg) on day 0 and after 1 and 2 wk, followed by 2% DSS in drinking water for the following week to induce preneoplastic lesions. The three experimental groups (Control, Hemin, and Hemin + EGCG) were treated for 6 wk. Hemin (2 g/kg) was orally administered daily and 0.1% EGCG was supplied in distilled water. (A) The experimental design for colon carcinogenesis in AOM/DSS mice. (B) Changes in body weight in mice treated with AOM/DSS, hemin, and EGCG. The body weight of all groups over time. (C) Tissue samples were stained with hematoxylin and eosin. All gross images are representative. Scale bars are 100 μm (magnification, ×100). (D) The total number of ACF in colon tissues was counted under a microscope (n = 15; $p < 0.001$: Control vs. Hemin; $p < 0.001$: Control vs. Hemin + EGCG). (E) The total number of AC in colonic tissues was counted under a microscope (n = 15; $p < 0.001$: Control vs. Hemin; $p = 0.001$: Control vs. Hemin + EGCG). (F) TBARS concentration was measured using a spectrophotometer to analyze lipid peroxidation in the feces (n = 8; $p < 0.001$: Control vs. Hemin; $p < 0.001$: Control vs. Hemin + EGCG). Quantitative data are presented as the mean ± SE of the mean with scatter plots.
AOM, azoxymethane; DSS, dextran sodium sulfate; EGCG, epigallocatechin-3-gallate; ICR, Institute for Cancer Research; ACF, aberrant crypt foci; AC, aberrant crypt; TBARS, thiobarbituric acid reactive substance.
*$p < 0.05$.

with the control group. In addition, TBARS concentration in the hemin + EGCG group was significantly decreased compared with the hemin group. Taken together, these data indicate that EGCG treatment suppressed hemin-induced colonic neoplasia as well as hemin-induced lipid peroxidation in the colonic mucosa of the AOM/DSS mouse model.

DISCUSSION

In this study, we evaluated the inhibitory effect of EGCG treatment on hemin-induced proliferation of Caco2 cells and colonic neoplastic change in an AOM/DSS model. Consistent with our findings, previous studies have suggested that heme incubation or biosynthesis is critical for tumorigenesis and the proliferation of colorectal cancer cells [20,21]. In addition to colorectal cancer, it has been reported that heme has a proliferative effect on other types of cancer. For example, in non-small-cell lung cancer, the inhibition of heme biosynthesis by succinyl acetone reduced the proliferation and survival of cancer cells [22]. Heme starvation by heme oxygenase resulted in an anti-proliferative effect on human breast cancer cells

[23]. Previous studies demonstrated that free heme and heme iron accumulation induced intracellular ROS accumulation, which caused DNA damage and gene mutation in colorectal cancer [24]. In addition, ROS-induced reactive lipid peroxides covalently bound to heme act as cytotoxic heme factors to induce damage to intestinal epithelial cells [25]. However, our data showed that various concentrations of hemin did not affect cell viability, although hemin significantly increased proliferation. This finding implies that the hemin-induced proliferative effect is important for colorectal cancer pathogenesis.

Furthermore, we observed that mitochondrial ROS is important for the hemin-induced proliferation of Caco2 cells. Studies have implicated mitochondrial ROS as a cancer promoter and a major therapeutic target for disrupting mitochondria-cell redox crosstalk [26]. Cancer-associated mitochondrial DNA mutations induce proton leaks which contribute to mitochondrial ROS generation in colon cancer [27]. However, the regulatory effect of heme or hemin on mitochondrial ROS generation in colorectal cancer has been poorly understood. In non-small cell lung cancer, the inhibition of heme biosynthesis decreased mitochondrial respiration, which suggests that hemin-induced mitochondrial ROS is closely associated with mitochondrial hyperactivation [22]. We further demonstrated that hemin-induced mitochondrial ROS increased hemin-induced Caco2 proliferation through the mitochondrial ROS scavenging assay. Similarly, previous studies found that the mitogenic effect of mitochondrial ROS is regulated by HIF1α stabilization and tumor suppressor gene inhibition [28]. The maintenance of mitochondrial redox balance is controlled by mitochondrial antioxidant enzymes including SOD2, GLRX2, thioredoxin, and thioredoxin reductase, which are necessary to prevent damage to cancer-associated biomolecules and processes [28]. Altogether, our results and that of previous studies indicate that mitochondrial ROS suppression may represent a therapeutic target for heme-associated colon carcinogenesis.

Although previous study has demonstrated that EGCG exhibits an anti-tumorigenic effect on colorectal cancer, the regulatory effect of EGCG on hemin-induced mitochondrial ROS accumulation has not been reported [29].

Our findings indicate that EGCG treatment decreases cellular proliferation by down-regulating mitochondrial ROS levels. Similarly, previous findings reported an anti-oxidative effect of EGCG treatment in various cell types [17,30]. Considering that hemin-induced Caco2 proliferation is mediated by mitochondrial ROS accumulation, EGCG-activated Nrf2 signaling reduces hemin-induced mitochondrial ROS levels and the proliferation of colorectal cancer cells, which is consistent with our findings.

We suggest that the stimulatory effect of hemin on Nrf2 expression as an adaptive response of hemin-induced oxidative stress. Previous study demonstrated that oxidative stress stimulating microenvironment increased expression levels of Nrf2 and Nrf2-associated anti-oxidant enzymes. Furthermore, the oxidative stress-induced Nrf2 signaling activation is an adaptive response which attenuates excessive ischemic damage and protects against environmental toxic effects and carcinogenesis [31]. Consistent with our finding, previous study also demonstrated that Nrf2 overexpression augmented hemin-induced thioredoxin expression for anti-oxidation [32]. Therefore, previous and our findings suggest that hemin-induced Nrf2 signaling acts as an adaptive response and EGCG treatment augmented hemin-induced Nrf2 signaling is critical for oxidative stress-stimulated colorectal carcinogenesis.

There have been several reports indicating a relationship between hemin treatment and Nrf2 signaling. For example, in human breast cancer cells, hemin treatment triggered JNK/Nrf2 signaling and heme oxygenase 1 (HO-1) activation [33]. In addition, hemin-induced Keap1/Nrf2 signaling activation is important for HO-1 induction in macrophages [34]. Similarly, our data showed a stimulatory effect of hemin on Nrf2 signaling and mitochondrial ROS accumulation. Therefore, we hypothesize that hemin-activated Nrf2 signaling is not sufficient for the suppression of hemin-induced mitochondrial ROS accumulation and proliferation of Caco2 cells. Furthermore, present study showed that long term (over 48 h) treatment of hemin significantly increased Nrf2 expression and mitochondrial ROS accumulation. EGCG treatment decreased Nrf2 expression through genomic pathway but not Keap1-mediated non-genomic pathway. Because the genomic pathway activation of EGCG regulated long term treatment of hemin-induced Nrf2 expression and mitochondrial ROS accumulation, both the data of both simultaneous and post- treatment of EGCG are similar to that of pretreatment of EGCG.

Previous studies showed a regulatory effect of EGCG treatment on mitochondrial antioxidant enzyme expression and proliferation of colorectal cancer cells [29,35]. EGCG-induced anti-oxidative stress is closely associated with the activation of Nrf2-targeted enzymes, such as SOD, GPX, and CAT [35]. Likewise, we demonstrated that EGCG treatment significantly enhanced hemin-induced Nrf2-targeted gene expression. According to previous reports, EGCG binds to the cysteine residues of Keap1 leading to the disruption of the Keap1-Nrf2 complex and Nrf2 stabilization [17]. Moreover, a previous report showed that EGCG treatment activated Nrf2 signaling, but did not alter Keap1 expression levels in a diabetic nephropathy model because of EGCG's mechanism of action [36]. Indeed, we confirmed that EGCG pretreatment did not affect Keap1 expression levels which were decreased by hemin treatment. Previous researchers oxidative stress-mediated GSK3β inhibition and PKC activation are critical for Keap1-independent Nrf2 signaling activation [37]. Although further study is needed for identification of detailed hemin and EGCG-regulated Nrf2 signaling pathway, we suggest that EGCG activates hemin-induced Nrf2 signaling through a Keap1-independent manner in colorectal cancer cells.

Our histological evidence supports the inhibitory effect of EGCG on hemin-induced neoplastic changes in colon tissue. Previous studies have shown that a heme iron and a heme iron-rich diet increase the number and the size of ACF and lipid peroxidation. This suggests that the effect of hemin-induced oxidative stress is important for hemin-induced colon carcinogenesis in the AOM/DSS model [38]. In addition, several studies demonstrated that hemin activates Wnt signaling to stimulate the hyperproliferation of colon epithelial cells through *APC* and β-catenin mutations, which leads to colon carcinogenesis [39]. Considering that Wnt signaling is closely associated with Nrf2 signaling, our data suggest that hemin-induced Wnt signaling directly regulates mitochondrial redox balance and cell proliferation [40]. Furthermore, our *in vivo* data confirm the inhibitory effect of EGCG supplementation on hemin-induced colorectal cancer pathogenesis and lipid peroxidation in the AOM/DSS model. Because the suppression of hemin-induced oxidative stress is a potential strategy to prevent colon tumor growth, our findings and that of others suggest that the regulatory effect of EGCG on ROS levels represent a rational anti-tumor treatment strategy [41,42]. In conclusion, we are the first to demonstrate that EGCG-induced Nrf2 signaling inhibits colon carcinogenesis through inhibition of mitochondrial ROS accumulation and cellular proliferation in vitro and in vivo. Furthermore, our findings suggest that EGCG supplementation is a preventive and therapeutic strategy to ameliorate heme–aggravated colon carcinogenesis.

SUPPLEMENTARY MATERIALS

Supplementary Table 1
Sequences of primers used for real-time polymerase chain reaction

Click here to view

Supplementary Fig. 1
Uncropped western blot images of **Fig. 1E**. Three representative uncropped blot images are described.

Click here to view

Supplementary Fig. 2
Uncropped western blot images of **Fig. 2D**. Three representative uncropped blot images are described.

Click here to view

Supplementary Fig. 3
Uncropped western blot images of **Fig. 3C**. Three representative uncropped blot images are described.

Click here to view

Supplementary Fig. 4
Uncropped western blot images of **Fig. 4A**. Three representative uncropped blot images are described.

Click here to view

Supplementary Fig. 5
Uncropped western blot images of **Fig. 4B**. Three representative uncropped blot images are described.

Click here to view

Supplementary Fig. 6
Uncropped western blot images of **Fig. 4E**. Three representative uncropped blot images are described.

Click here to view

Supplementary Fig. 7
Effects of pre, simultaneous and post treatments with EGCG on hemin-induced proliferation and mitochondrial ROS accumulation of Caco2 cells. (A, B) Caco2 cells were incubated with hemin (1 μM) and EGCG (1 μM, pre, simultaneous, and post treatments) for 48 h. (A) WST-1 levels were measured by the WST-1 cell proliferation assay (n = 9; $p < 0.001$: Control vs. Hemin; $p = 0.003$: Hemin vs. Hemin + EGCG pretreatment; $p = 0.003$: Hemin vs. Hemin +

EGCG simultaneous treatment; p = 0.003: Hemin vs. Hemin + EGCG post treatment). (B) Mitochondrial ROS levels were analyzed by the MitoSOX staining assay (n = 9; p < 0.001: Control vs. Hemin; p = 0.004: Hemin vs. Hemin + EGCG pretreatment; p = 0.004: Hemin vs. Hemin + EGCG simultaneous treatment; p = 0.011: Hemin vs. Hemin + EGCG post treatment).

Click here to view

Supplementary Fig. 8

Effect of trigonelline on hemin-increased mitochondrial ROS accumulation. Caco2 cells were pretreated with trigonelline (10 μM) for 30 min prior to hemin (1 μM) for 48 h. Mitochondrial ROS levels were measured by MitoSOX staining assay (n = 9; p = 0.037: Control vs. Hemin; p = 0.044: Hemin vs. Hemin + Trigonelline; p = 0.014: Control vs. Trigonelline).

Click here to view

REFERENCES

1. Seiwert N, Heylmann D, Hasselwander S, Fahrer J. Mechanism of colorectal carcinogenesis triggered by heme iron from red meat. Biochim Biophys Acta Rev Cancer. 2020;1873(1):188334.
   PUBMED | **CROSSREF**

2. Gamage SM, Dissabandara L, Lam AK, Gopalan V. The role of heme iron molecules derived from red and processed meat in the pathogenesis of colorectal carcinoma. Crit Rev Oncol Hematol. 2018;126:121-128.
   PUBMED | **CROSSREF**

3. Wiseman M. The second World Cancer Research Fund/American Institute for Cancer Research expert report. Food, nutrition, physical activity, and the prevention of cancer: a global perspective. Proc Nutr Soc. 2008;67(3):253-256.
   PUBMED | **CROSSREF**

4. Bastide NM, Pierre FH, Corpet DE. Heme iron from meat and risk of colorectal cancer: a meta-analysis and a review of the mechanisms involved. Cancer Prev Res (Phila). 2011;4(2):177-184.
   PUBMED | **CROSSREF**

5. Sesink AL, Termont DS, Kleibeuker JH, Van der Meer R. Red meat and colon cancer: the cytotoxic and hyperproliferative effects of dietary heme. Cancer Res 1999;59(22):5704-5709.
   PUBMED

6. Pierre F, Taché S, Petit CR, Van der Meer R, Corpet DE. Meat and cancer: haemoglobin and haemin in a low-calcium diet promote colorectal carcinogenesis at the aberrant crypt stage in rats. Carcinogenesis. 2003;24(10):1683-1690.
   PUBMED | **CROSSREF**

7. Fiorito V, Chiabrando D, Petrillo S, Bertino F, Tolosano E. The multifaceted role of heme in cancer. Front Oncol. 2020;9:1540.
   PUBMED | **CROSSREF**

8. Sødring M, Oostindjer M, Egelandsdal B, Paulsen JE. Effects of hemin and nitrite on intestinal tumorigenesis in the A/J Min/+ mouse model. PLoS One. 2015;10(4):e0122880.
   PUBMED | **CROSSREF**

9. Sesink AL, Termont DS, Kleibeuker JH, Van Der Meer R. Red meat and colon cancer: dietary haem, but not fat, has cytotoxic and hyperproliferative effects on rat colonic epithelium. Carcinogenesis. 2000;21(10):1909-1915.
   PUBMED | **CROSSREF**

10. Cheng Z, Li Y. What is responsible for the initiating chemistry of iron-mediated lipid peroxidation: an update. Chem Rev. 2007;107(3):748-766.
    PUBMED | **CROSSREF**

11. Gaschler MM, Stockwell BR. Lipid peroxidation in cell death. Biochem Biophys Res Commun. 2017;482(3):419-425.
    PUBMED | **CROSSREF**

12. Tappel A. Heme of consumed red meat can act as a catalyst of oxidative damage and could initiate colon, breast and prostate cancers, heart disease and other diseases. Med Hypotheses. 2007;68(3):562-564.
    PUBMED | CROSSREF

13. Kim HS, Quon MJ, Kim JA. New insights into the mechanisms of polyphenols beyond antioxidant properties; lessons from the green tea polyphenol, epigallocatechin 3-gallate. Redox Biol. 2014;2:187-195.
    PUBMED | CROSSREF

14. Eng QY, Thanikachalam PV, Ramamurthy S. Molecular understanding of epigallocatechin gallate (EGCG) in cardiovascular and metabolic diseases. J Ethnopharmacol. 2018;210:296-310.
    PUBMED | CROSSREF

15. Kuriyama S, Shimazu T, Ohmori K, Kikuchi N, Nakaya N, Nishino Y, et al. Green tea consumption and mortality due to cardiovascular disease, cancer, and all causes in Japan: the Ohsaki study. JAMA. 2006;296(10):1255-1265.
    PUBMED | CROSSREF

16. Meng Q, Velalar CN, Ruan R. Regulating the age-related oxidative damage, mitochondrial integrity, and antioxidative enzyme activity in Fischer 344 rats by supplementation of the antioxidant epigallocatechin-3-gallate. Rejuvenation Res. 2008;11(3):649-660.
    PUBMED | CROSSREF

17. Na HK, Surh YJ. Modulation of Nrf2-mediated antioxidant and detoxifying enzyme induction by the green tea polyphenol EGCG. Food Chem Toxicol. 2008;46(4):1271-1278.
    PUBMED | CROSSREF

18. La X, Zhang L, Li Z, Li H, Yang Y. (-)-Epigallocatechin gallate (EGCG) enhances the sensitivity of colorectal cancer cells to 5-FU by inhibiting GRP78/NF-κB/miR-155-5p/MDR1 pathway. J Agric Food Chem. 2019;67(9):2510-2518.
    PUBMED | CROSSREF

19. Lee HJ, Jung YH, Choi GE, Ko SH, Lee SJ, Lee SH, et al. BNIP3 induction by hypoxia stimulates FASN-dependent free fatty acid production enhancing therapeutic potential of umbilical cord blood-derived human mesenchymal stem cells. Redox Biol. 2017;13:426-443.
    PUBMED | CROSSREF

20. Kruger C, Zhou Y. Red meat and colon cancer: a review of mechanistic evidence for heme in the context of risk assessment methodology. Food Chem Toxicol. 2018;118:131-153.
    PUBMED | CROSSREF

21. Fiorito V, Allocco AL, Petrillo S, Gazzano E, Torretta S, Marchi S, et al. The heme synthesis-export system regulates the tricarboxylic acid cycle flux and oxidative phosphorylation. Cell Reports. 2021;35(11):109252.
    PUBMED | CROSSREF

22. Hooda J, Cadinu D, Alam MM, Shah A, Cao TM, Sullivan LA, et al. Enhanced heme function and mitochondrial respiration promote the progression of lung cancer cells. PLoS One. 2013;8(5):e63402.
    PUBMED | CROSSREF

23. Hill M, Pereira V, Chauveau C, Zagani R, Remy S, Tesson L, et al. Heme oxygenase-1 inhibits rat and human breast cancer cell proliferation: mutual cross inhibition with indoleamine 2,3-dioxygenase. FASEB J. 2005;19(14):1957-1968.
    PUBMED | CROSSREF

24. IJssennagger N, Rijnierse A, de Wit N, Jonker-Termont D, Dekker J, Müller M, et al. Dietary haem stimulates epithelial cell turnover by downregulating feedback inhibitors of proliferation in murine colon. Gut. 2012;61(7):1041-1049.
    PUBMED | CROSSREF

25. Ijssennagger N, Rijnierse A, de Wit NJ, Boekschoten MV, Dekker J, Schonewille A, et al. Dietary heme induces acute oxidative stress, but delayed cytotoxicity and compensatory hyperproliferation in mouse colon. Carcinogenesis. 2013;34(7):1628-1635.
    PUBMED | CROSSREF

26. Sabharwal SS, Schumacker PT. Mitochondrial ROS in cancer: initiators, amplifiers or an Achilles' heel? Nat Rev Cancer. 2014;14(11):709-721.
    PUBMED | CROSSREF

27. Namslauer I, Brzezinski P. A mitochondrial DNA mutation linked to colon cancer results in proton leaks in cytochrome c oxidase. Proc Natl Acad Sci U S A. 2009;106(9):3402-3407.
    PUBMED | CROSSREF

28. Idelchik MD, Begley U, Begley TJ, Melendez JA. Mitochondrial ROS control of cancer. Semin Cancer Biol. 2017;47:57-66.
    PUBMED | CROSSREF

29. Luo KW, Xia J, Cheng BH, Gao HC, Fu LW, Luo XL. Tea polyphenol EGCG inhibited colorectal-cancer-cell proliferation and migration via downregulation of STAT3. Gastroenterol Rep (Oxf). 2021;9(1):59-70.
   PUBMED | CROSSREF

30. Cia D, Vergnaud-Gauduchon J, Jacquemot N, Doly M. Epigallocatechin gallate (EGCG) prevents H_2O_2-induced oxidative stress in primary rat retinal pigment epithelial cells. Curr Eye Res. 2014;39(9):944-952.
   PUBMED | CROSSREF

31. Osburn WO, Kensler TW. Nrf2 signaling: an adaptive response pathway for protection against environmental toxic insults. Mutat Res. 2008;659(1-2):31-39.
   PUBMED | CROSSREF

32. Kim YC, Masutani H, Yamaguchi Y, Itoh K, Yamamoto M, Yodoi J. Hemin-induced activation of the thioredoxin gene by Nrf2. A differential regulation of the antioxidant responsive element by a switch of its binding factors. J Biol Chem. 2001;276(21):18399-18406.
   PUBMED | CROSSREF

33. Jang HY, Hong OY, Chung EY, Park KH, Kim JS. Roles of JNK/Nrf2 pathway on hemin-induced heme oxygenase-1 activation in MCF-7 human breast cancer cells. Medicina (Kaunas). 2020;56(6):268.
   PUBMED | CROSSREF

34. Boyle JJ, Johns M, Lo J, Chiodini A, Ambrose N, Evans PC, et al. Heme induces heme oxygenase 1 via Nrf2: role in the homeostatic macrophage response to intraplaque hemorrhage. Arterioscler Thromb Vasc Biol. 2011;31(11):2685-2691.
   PUBMED | CROSSREF

35. Han XD, Zhang YY, Wang KL, Huang YP, Yang ZB, Liu Z. The involvement of Nrf2 in the protective effects of (-)-epigallocatechin-3-gallate (EGCG) on NaAsO$_2$-induced hepatotoxicity. Oncotarget. 2017;8(39):65302-65312.
   PUBMED | CROSSREF

36. Sun W, Liu X, Zhang H, Song Y, Li T, Liu X, et al. Epigallocatechin gallate upregulates NRF2 to prevent diabetic nephropathy via disabling KEAP1. Free Radic Biol Med. 2017;108:840-857.
   PUBMED | CROSSREF

37. Baumel-Alterzon S, Katz LS, Brill G, Garcia-Ocaña A, Scott DK. Nrf2: the master and captain of beta cell fate. Trends Endocrinol Metab. 2021;32(1):7-19.
   PUBMED | CROSSREF

38. Pierre FH, Santarelli RL, Allam O, Tache S, Naud N, Gueraud F, et al. Freeze-dried ham promotes azoxymethane-induced mucin-depleted foci and aberrant crypt foci in rat colon. Nutr Cancer. 2010;62(5):567-573.
   PUBMED | CROSSREF

39. Radulescu S, Brookes MJ, Salgueiro P, Ridgway RA, McGhee E, Anderson K, et al. Luminal iron levels govern intestinal tumorigenesis after *Apc* loss in vivo. Cell Reports. 2016;17(10):2805-2807.
   PUBMED | CROSSREF

40. Rada P, Rojo AI, Offergeld A, Feng GJ, Velasco-Martín JP, González-Sancho JM, et al. WNT-3A regulates an Axin1/NRF2 complex that regulates antioxidant metabolism in hepatocytes. Antioxid Redox Signal. 2015;22(7):555-571.
   PUBMED | CROSSREF

41. Kim H, Yin K, Falcon DM, Xue X. The interaction of Hemin and Sestrin2 modulates oxidative stress and colon tumor growth. Toxicol Appl Pharmacol. 2019;374:77-85.
   PUBMED | CROSSREF

42. Kwak TW, Park SB, Kim HJ, Jeong YI, Kang DH. Anticancer activities of epigallocatechin-3-gallate against cholangiocarcinoma cells. Onco Targets Ther. 2016;10:137-144.
   PUBMED | CROSSREF